number of A alleles of −123 C/A SNP, T alleles of −88 G/T SNP, and A alleles of +20 C/A SNP carried by HBE cells according to a simple regression analysis ($p=0.013$, $p=0.0035$, and $p<0.0001$, respectively) (Fig. 4b). Multiple regression analysis showed that the association of +20 C/A SNP remained significant ($p=0.016$), whereas the association of −123 C/A and −88 G/T SNPs was insignificant ($p=0.67$ and $p=0.78$, respectively). In contrast, baseline expression of the T0 transcript was slightly higher in proportion to the number of C alleles of −77 C/G SNP; however, this increase was not statistically significant ($p=0.086$) (Fig. 4a).

When the relative expression of the total MxA transcripts was compared with expression of the T1 and T0 transcripts under the unstimulated condition, the overall expression of MxA strongly correlated with expression of the T1 transcript (Spearman's rank correlation coefficient; rs=0.759), whereas it weakly correlated with expression of the T0 transcript (rs=0.388). The total expression of MxA was significantly higher in proportion to the number of −123 A, −88 T, and −20 A alleles ($p=0.0004$, $p<0.0001$, and $p<0.0001$, respectively), which was similar to the linear relationship between the T1 transcript and number of alleles shown above.

When immortalized HBE cell line BEAS-2B was stimulated with poly(I:C), time-course analysis revealed that expression of the T0 transcript was the highest after 24 h, whereas that of the T1 transcript was the highest after 6–12 h of incubation (Online Resource 3). We therefore investigated the expression of T0 and T1 transcripts in HBE cells ($n=29$) stimulated with poly(I:C) for 24 h. The expression of the T0 transcript increased eightfold, whereas that of the T1 transcript increased 870-fold. Poly(I:C)-induced expression of both transcripts was not associated with either allele of the four SNPs (Fig. 5a, b). When HBE cells ($n=9$) were stimulated with IFN-β for 12 h, the T0 transcript was induced eightfold, and the T1 transcript was induced 640-fold. IFN-β-induced expression of the transcripts did not vary among genotypes (data not shown).

Discussion

In this study, we investigated the expression profile of MxA by analyzing expression of the original transcript T1 and the transcript variant T0 in primary cultured HBE cells. According to our absolute quantification method using real-time RT-PCR, the amount of the T0 transcript was approximately half of that of the T1 transcript at the baseline level. Although expression of the T0 transcript was also induced by type I IFNs and poly(I:C) and its 5′ proximal region has a potential ISRE motif, IFN-β and poly(I:C) inducibility of the T1 transcript was at least 100-fold higher than that of the

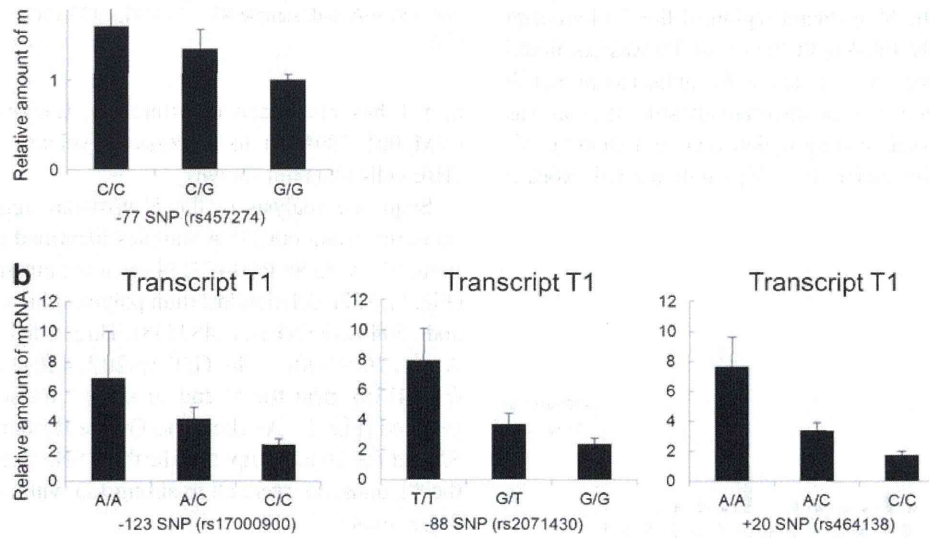

Fig. 4 Differences in the baseline expression of transcript variants among the genotypes of the promoter and exon 1 SNPs in HBE cells. Expression of **a** T0 and **b** T1 transcripts under the unstimulated condition in HBE cells with each genotype of −77 C/G SNP for the T0 transcript (C/C, $n=8$; C/G, $n=18$; G/G, $n=12$), of −123 C/A SNP (A/A, $n=2$; A/C, $n=18$; C/C, $n=18$), of −88 G/T SNP (T/T, $n=3$; G/T, $n=19$; G/G, $n=16$), and of +20 C/A SNP (A/A, $n=5$; A/C, $n=22$; C/C, $n=11$) for the T1 transcript is shown. The relative amounts of mRNA of each transcript compared with that of the T0 transcript in GG cells without poly(I:C) stimulation are shown as mean±SEM. Possible associations between the number of alleles and the amount of the corresponding transcripts were assessed by a simple regression model respectively ($p=0.086$ for the number of −77 C alleles, $p=0.013$ for −123 A alleles, $p=0.0035$ for −88 T alleles, and $p<0.0001$ for +20 A alleles)

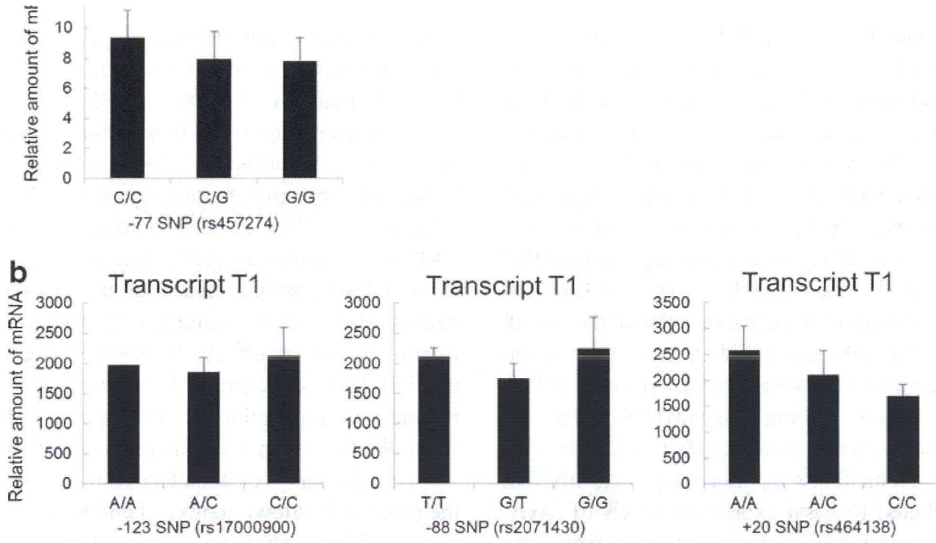

Fig. 5 Differences in the poly(I:C)-induced expression of transcript variants among the genotypes of the promoter and exon 1 SNPs in HBE cells. Expression of **a** T0 and **b** T1 transcripts in the presence of poly(I:C) in HBE cells with each genotype of −77 C/G SNP for the T0 transcript (C/C, $n=5$; C/G, $n=13$; G/G, $n=11$), of −123 C/A SNP (A/A, $n=1$; A/C, $n=12$; C/C, $n=16$), of −88 G/T SNP (T/T, $n=2$; G/T, $n=13$; G/G, $n=14$), and of +20 C/A SNP (A/A, $n=3$; A/C, $n=16$; C/C, $n=10$) for the T1 transcript is shown. The relative amounts of mRNA of each transcript compared with that of the T0 transcript in GG cells without poly(I:C) stimulation are shown as mean±SEM. Possible associations were assessed by a simple regression model ($p=0.647$ for the number of −77 C alleles, $p=0.662$ for −123 A alleles, $p=0.539$ for −88 T alleles, and $p=0.331$ for +20 A alleles)

T0 transcript. This observation implies that MxA response to viral infection of respiratory cells is mostly controlled by the expression of the T1 transcript.

Remarkably increased levels of the T1 transcript after stimulation with type I IFNs or an IFN-inducing agent, poly(I:C), were consistent with the general consensus that the induction of MxA requires type I or type III IFN signaling (Haller and Kochs 2011). However, levels of the T1 transcript were also elevated in HBE cells by other physiological stimuli. Moderate elevation of levels of the T1 transcript in the presence of IFN-γ and TNF-α may be mediated by the secondary induction of type I or type III IFNs. Although Mahanonda et al. (2012) demonstrated the induction of MxA by α-defensin in primary human gingival epithelial cells, the mechanism by which the T1 transcript was upregulated by α-defensin remains unknown. These observations support the idea that the T1 transcript plays a major role in airway diseases.

We also analyzed the expression of T0 transcript with alternative 5′ untranslated exons. Alternative promoter usage is now recognized as a common mechanism in the transcriptional regulation of mammalian genes (Davuluri et al. 2008). Among IFN-stimulated genes, ADAR1 was shown to have alternative promoters (George and Samuel 1999): one promoter contributes to constitutive expression and the other to inducible expression. To our knowledge, no IFN-stimulated genes other than MxA, whose antiviral function is well known (Sadler and Williams 2008), have been reported to possess two IFN-inducible transcripts with distinct first exons. The molecular mechanism for tissue specificity of these transcripts is unknown; however, of note, the promoter of the T0 transcript contains the putative steroidogenic factor-1 binding site (position −636 to −644) thought to be important to testis- and adrenal gland-specific gene expression (Schimmer and White 2010). A study of the expression profiles of MxA in various organs would be interesting.

Although IFN-mediated upregulation of the T0 transcript was moderate in contrast to that of the T1 transcript, baseline levels of the T0 transcript were not negligible in HBE cells. It is thus conceivable that the T0 transcript plays a minor but independent role in the human airway. Furthermore, considering the difference between the time course of mRNA expression of the T0 and T1 transcripts after poly(I:C) stimulation, it is likely that other factors further modulate their induction levels. Because some reports (Aebi et al. 1989; Goetschy et al. 1989; Prescott et al. 2005) indicate the presence of IFN-independent induction of MxA in contrast to the results of Holzinger et al. (2007), it would be worth investigating whether the T0 transcript can be induced through an IFN-independent signaling system in viral infection.

We observed the regulatory effects of −123, −88, and −20 SNPs on mRNA levels of the T1 transcript in HBE cells

under the unstimulated condition. When we evaluated the overall expression of the MxA transcripts by real-time RT-PCR, it was found to be closely correlated with levels of the T1 transcript, suggesting that individual variation of the total expression of MxA is mainly explained by the T1 transcript. Indeed overall levels of MxA as well as expression of the T1 transcript were strongly associated with these three SNPs at baseline levels. It has been repeatedly reported that the minor A allele of −123 SNP and the minor T allele of −88 SNP, which are in strong LD, were associated with the overall transcriptional activity of the gene (Hijikata et al. 2001; Torisu et al. 2004). Expression of MxA was associated with −88 G/T SNP when PBMC cells were stimulated with IFN-α2 for 12 h (Fernandez-Arcas et al. 2004). In one study (Furuyama et al. 2006), the results of a luciferase reporter assay suggested that −123 SNP contributed to basal expression levels of MxA, whereas −88 SNP contributed to the induction of expression by IFNs. Ching et al. (2010) further showed that the −123A allele had a stronger binding affinity to nuclear proteins from unstimulated cells and that the −88 T allele preferentially bound to the protein after IFN-β stimulation. In our study using HBE cells, −123, −88, and −20 SNPs were all associated with baseline expression of the T1 transcript, and according to a multiple regression analysis, among the three SNPs, +20 C/A SNP was still associated with baseline expression of the T1 transcript. This finding may be attributed to the difference in cell type; however, extensive investigation is required to determine the possible effect of +20 SNP or other unknown functional polymorphisms in strong LD. Recently, Tran Thi Duc et al. (2012) reported that three SNPs (−309 C/G, −101 G/A, and +20 C/A) also contributed to the promoter activity in combination with well-known effects of −123 and −88 SNPs. We could not examine −309 and −101 SNPs in our samples because −309 C/G and −101 G/A SNPs were detected only in the African population and their minor allele frequencies were relatively low (Duc et al. 2012).

Under the poly(I:C)-stimulated condition, the −20 SNP also tended to be associated with expression of the T1 transcript in our study; however, this tendency was not statistically significant. When HBE cells were stimulated with IFN-β for 12 h, the same three SNPs were not associated with the expression level. These findings may conflict with the in vitro effects of these 5′ SNPs on the IFN-inducible promoter activity previously assessed by a luciferase reporter system (Hijikata et al. 2001; Torisu et al. 2004; Tran Thi Duc et al. 2012). In our study, however, the mRNA induced by poly (I:C), the dsRNA analog to mimic viral infection, was directly assessed in primary cultured HBE cells, which implies that individual variance of relevant factors such as toll-like receptor 3 and subsequent IFN signaling pathways might have affected the mRNA levels in the IFN-stimulated condition and have masked the independent effects of these promoter SNPs of the MxA gene.

We previously reported that the promoter −88 SNP was associated with severity of SARS in the Vietnamese population (Hamano et al. 2005), and the promoter −123 SNP was associated with SARS in the Chinese population (Ching et al. 2010). According to Chen and Subbarao (2007), IFN induction is completely suppressed in SARS coronavirus-infected cells. Our ex vivo findings that these regulatory SNPs were mainly involved in baseline expression of the T1 transcript support the results of these disease association studies. However, we could not show significant difference in the regulatory effects between −88 and −123 SNPs, possibly because of strong LD between these two SNPs in the Japanese population (r^2=0.83) compared with moderate LD in the Chinese population (r^2=0.39) (Ching et al. 2010).

In conclusion, we characterized the expression profile of the previously known transcript and the transcript variant of MxA and demonstrated a significant effect of its 5′ SNPs on basal expression of the overall transcripts in HBE cells. Our findings may lead to an improved understanding of the association of MxA SNPs with susceptibility to respiratory viral infections.

Acknowledgments We thank Keiko Wakabayashi for technical assistance in the study. This work was partly supported by a grant from the National Center for Global Health and Medicine.

Conflict of interest All authors have no conflict of interest on this work.

References

Abe H, Hayes CN, Ochi H, Maekawa T, Tsuge M, Miki D, Mitsui F, Hiraga N, Imamura M, Takahashi S, Kubo M, Nakamura Y, Chayama K (2011) IL28 variation affects expression of interferon stimulated genes and peg-interferon and ribavirin therapy. J Hepatol 54:1094–1101

Aebi M, Fah J, Hurt N, Samuel CE, Thomis D, Bazzigher L, Pavlovic J, Haller O, Staeheli P (1989) cDNA structures and regulation of two interferon-induced human Mx proteins. Mol Cell Biol 9:5062–5072

Barrett JC, Fry B, Maller J, Daly MJ (2005) Haploview: analysis and visualization of LD and haplotype maps. Bioinformatics 21:263–265

Chen J, Subbarao K (2007) The immunobiology of SARS. Annu Rev Immunol 25:443–472

Ching JC, Chan KY, Lee EH, Xu MS, Ting CK, So TM, Sham PC, Leung GM, Peiris JS, Khoo US (2010) Significance of the myxovirus resistance A (MxA) gene −123C>a single-nucleotide polymorphism in suppressed interferon beta induction of severe acute respiratory syndrome coronavirus infection. J Infect Dis 201:1899–1908

Davuluri RV, Suzuki Y, Sugano S, Plass C, Huang TH (2008) The functional consequences of alternative promoter use in mammalian genomes. Trends Genet 24:167–177

Duc TT, Famir F, Michaux C, Desmecht D, Cornet A (2012) Detection of new biallelic polymorphisms in the human MxA gene. Mol Biol Rep 39:8533–8538

Fernandez-Arcas N, Blanco A, Gaitan MJ, Nyqvist M, Alonso A, Reyes-Engel A (2004) Differential transcriptional expresion of

the polymorphic myxovirus resistance protein A in response to interferon-alpha treatment. Pharmacogenetics 14:189–193
Furuyama H, Chiba S, Okabayashi T, Yokota S, Nonaka M, Imai T, Fujii N, Matsumoto H (2006) Single nucleotide polymorphisms and functional analysis of MxA promoter region in multiple sclerosis. J Neurol Sci 249:153–157
George CX, Samuel CE (1999) Human RNA-specific adenosine deaminase ADAR1 transcripts possess alternative exon 1 structures that initiate from different promoters, one constitutively active and the other interferon inducible. Proc Natl Acad Sci U S A 96:4621–4626
Goetschy JF, Zeller H, Content J, Horisberger MA (1989) Regulation of the interferon-inducible IFI-78K gene, the human equivalent of the murine Mx gene, by interferons, double-stranded RNA, certain cytokines, and viruses. J Virol 63:2616–2622
Gray TE, Guzman K, Davis CW, Abdullah LH, Nettesheim P (1996) Mucociliary differentiation of serially passaged normal human tracheobronchial epithelial cells. Am J Respir Cell Mol Biol 14:104–112
Haller O, Kochs G (2011) Human MxA protein: an interferon-induced dynamin-like GTPase with broad antiviral activity. J Interferon Cytokine Res 31:79–87
Hamano E, Hijikata M, Itoyama S, Quy T, Phi NC, Long HT, Ha LD, Ban VV, Matsushita I, Yanai H, Kirikae F, Kirikae T, Kuratsuji T, Sasazuki T, Keicho N (2005) Polymorphisms of interferon-inducible genes OAS-1 and MxA associated with SARS in the Vietnamese population. Biochem Biophys Res Commun 329:1234–1239
Hijikata M, Mishiro S, Miyamoto C, Furuichi Y, Hashimoto M, Ohta Y (2001) Genetic polymorphism of the MxA gene promoter and interferon responsiveness of hepatitis C patients: revisited by analyzing two SNP sites (−123 and −88) in vivo and in vitro. Intervirology 44:379–382
Hijikata M, Ohta Y, Mishiro S (2000) Identification of a single nucleotide polymorphism in the MxA gene promoter (G/T at nt −88) correlated with the response of hepatitis C patients to interferon. Intervirology 43:124–127
Holzinger D, Jorns C, Stertz S, Boisson-Dupuis S, Thimme R, Weidmann M, Casanova JL, Haller O, Kochs G (2007) Induction of MxA gene expression by influenza A virus requires type I or type III interferon signaling. J Virol 81:7776–7785
Horisberger MA, McMaster GK, Zeller H, Wathelet MG, Dellis J, Content J (1990) Cloning and sequence analyses of cDNAs for interferon- and virus-induced human Mx proteins reveal that they contain putative guanine nucleotide-binding sites: functional study of the corresponding gene promoter. J Virol 64:1171–1181
Kong XF, Zhang XX, Gong QM, Gao J, Zhang SY, Wang L, Xu J, Han Y, Jin GD, Jiang JH, Zhang DH, Lu ZM (2007) MxA induction may predict sustained virologic responses of chronic hepatitis B patients with IFN-alpha treatment. J Interferon Cytokine Res 27:809–818
Leong DT, Gupta A, Bai HF, Wan G, Yoong LF, Too HP, Chew FT, Hutmacher DW (2007) Absolute quantification of gene expression in biomaterials research using real-time PCR. Biomaterials 28:203–210
Mahanonda R, Sa-Ard-Iam N, Rerkyen P, Thitithanyanont A, Subbalekha K, Pichyangkul S (2012) MxA expression induced by alpha-defensin in healthy human periodontal tissue. Eur J Immunol 42:946–956
McGilvray I, Feld JJ, Chen L, Pattullo V, Guindi M, Fischer S, Borozan I, Xie G, Selzner N, Heathcote EJ, Siminovitch K (2012) Hepatic cell-type specific gene expression better predicts HCV treatment outcome than IL28B genotype. Gastroenterology 142:1122–1131
Peng XM, Lei RX, Gu L, Ma HH, Xie QF, Gao ZL (2007) Influences of MxA gene −88 G/T and IFN-gamma +874 A/T on the natural history of hepatitis B virus infection in an endemic area. Int J Immunogenet 34:341–346
Prescott J, Ye C, Sen G, Hjelle B (2005) Induction of innate immune response genes by Sin Nombre hantavirus does not require viral replication. J Virol 79:15007–15015
Randall RE, Goodbourn S (2008) Interferons and viruses: an interplay between induction, signalling, antiviral responses and virus countermeasures. J Gen Virol 89:1–47
Ronni T, Matikainen S, Lehtonen A, Palvimo J, Dellis J, Van Eylen F, Goetschy JF, Horisberger M, Content J, Julkunen I (1998) The proximal interferon-stimulated response elements are essential for interferon responsiveness: a promoter analysis of the antiviral MxA gene. J Interferon Cytokine Res 18:773–781
Sadler AJ, Williams BR (2008) Interferon-inducible antiviral effectors. Nat Rev Immunol 8:559–568
Schimmer BP, White PC (2010) Minireview: steroidogenic factor 1: its roles in differentiation, development, and disease. Mol Endocrinol 24:1322–1337
Torisu H, Kusuhara K, Kira R, Bassuny WM, Sakai Y, Sanefuji M, Takemoto M, Hara T (2004) Functional MxA promoter polymorphism associated with subacute sclerosing panencephalitis. Neurology 62:457–460
Tran Thi Duc T, Desmecht D, Cornet A (2012) Functional characterization of new allelic polymorphisms identified in the promoter region of the human MxA gene. Int J Immunogenet. doi:10.1111/j.1744-313X.2012.01153.x

The Journal of Toxicological Sciences (J. Toxicol. Sci.)
Vol.38, No.4, 619-628, 2013

Original Article

An improved dispersion method of multi-wall carbon nanotube for inhalation toxicity studies of experimental animals

Yuhji Taquahashi, Yukio Ogawa, Atsuya Takagi, Masaki Tsuji, Koichi Morita and Jun Kanno

Division of Cellular and Molecular Toxicology, Biological Safety Research Center, National Institute of Health Sciences, 1-18-1 Kamiyoga, Setagaya-ku, Tokyo 158-8501, Japan

(Received May 5, 2013; Accepted June 9, 2013)

ABSTRACT — A multi-wall carbon nanotube (MWCNT) product Mitsui MWNT-7 is a mixture of dispersed single fibers and their agglomerates/aggregates. In rodents, installation of such mixture induces inflammatory lesions triggered predominantly by the aggregates/agglomerates at the level of terminal bronchiole of the lungs. In human, however, pulmonary toxicity induced by dispersed single fibers that reached the lung alveoli is most important to assess. Therefore, a method to generate aerosol predominantly consisting of dispersed single fibers without changing their length and width is needed for inhalation studies. Here, we report a method (designated as Taquann method) to effectively remove the aggregate/agglomerates and enrich the well-dispersed singler fibers in dry state without dispersant and without changing the length and width distribution of the single fibers. This method is base on two major concept; liquid-phase fine filtration and critical point drying to avoid re-aggregation by surface tension. MWNT-7 was suspended in Tert-butyl alcohol, freeze-and-thawed, filtered by a vibrating 25 μm mesh Metallic Sieve, snap-frozen by liquid nitrogen, and vacuum-sublimated (an alternative method to carbon dioxide critical point drying). A newly designed direct injection system generated well-dispersed aerosol in an inhalation chamber. The lung of mice exposed to the aerosol contained single fibers with a length distribution similar to the original and the Taquann-treated sample. Taquann method utilizes inexpensive materials and equipments mostly found in common biological laboratories, and prepares dry powder ready to make well-dispersed aerosol. This method and the chamber with direct injection system would facilitate the inhalation toxicity studies more relevant to human exposure.

Key words: Multi-wall carbon nanotube, Dispersion, Metallic sieve, Tert-butyl alcohol, Sublimation, Critical point drying

INTRODUCTION

We previously reported that a certain make of multi-wall carbon nanotube (MWCNT) contained particles similar to asbestos fibers in size and shape, and was positive for mesotheliomagenesis in intraperitoneal injection studies using p53-heterozygous mice (Takagi *et al.*, 2008, 2012). The intraperitoneal injection study is a specialized method for the detection of mesotheliomagenic potential of inhaled fibrous materials (Pott *et al.*, 1994; Roller *et al.*, 1997; Poland *et al.*, 2008). For the assessment of general respiratory toxicity including non-cancerous endpoints, the inhalation studies are considered essential. As a surrogate for inhalation studies, pharyngeal aspiration and intratracheal spray methods are often used. However, in both methods, the suspension medium may modify the distribution and/or the toxicity of the test particles (Morimoto *et al.*, 2011; Oyabu *et al.*, 2011; Gasser *et al.*, 2012; Wang *et al.*, 2012). Dispersion methods without suspension media are reported. However, those are usually using, at least in part of the processes, rigorous sonication or mechanical milling resulting in certain degree of physiological changes in sample characteristics, such as shortening in length distribution of MWNCT (Muller *et al.*, 2005; Mitchell *et al.*, 2007; Ahn *et al.*, 2011). Changes in particle size and/or shape will also affect the nature

Correspondence: Jun Kanno (E-mail: kanno@nihs.go.jp)

and strength of toxicity of the test substances. Therefore, development of a dispersion method to generate the aerosol of concern without addition of chemicals and changes in particle dimensions is considered to be essential for the assessment of inhalation toxicity in humans.

Fibrous nanomaterial such as Mitsui MWNT-7 is a mixture of dispersed single fibers of various length and width, and their agglomerates and aggregates. When given as a mixture, the lung lesions were mainly seen as inflammatory and/or granulomatous lesions with various degree of fibrosis at the level of terminal bronchiole accompanying the aggregates and agglomerates. These lesions were considered to block and/or mask the changes induced by the single fibers that should have reached the alveolar ducts and alveoli (Warheit *et al.*, 2004; Muller *et al.*, 2005; Shvedova *et al.*, 2008; Porter *et al.*, 2009; Mercer *et al.*, 2011; Wang *et al.*, 2011). Therefore, assessment of the toxicity of single fibers needs well-dispersed sample without aggregate/agglomerate. In practical inhalation testing, the animal chamber air is rigorously agitated in order to ensure the homogeneity of aerosol in the chamber. Therefore, if the MWNT-7 as a mixture is used, the likelihood of aggregates/agglomerates reaching the nose of the animals is high. In contrast, human ambient air is less agitated; the aggregates/agglomerates may sediment away fast and dispersed single fibers may stay longer in the air to be inhaled by humans (Han *et al.*, 2008). In addition, humans have longer respiratory tract compared to rodents and may effectively filtered out aggregates/agglomerates before the air reaches the alveolar region.

Taking all into account, we concluded that it is essential to prepare a dispersed single fiber aerosol without aggregate/agglomerates, without additional chemical components, and without changes in size and shape of the single fiber component for the rodent inhalation studies in order to predict human inhalation toxicity. To date, one dispersion method is reported, i.e. the filtration system. Filtration by a sieve with its pore size smaller than the size of aggregates/agglomerate will not affect the size distribution of the single fibers (Kasai *et al.*, 2013). However, filtration in gaseous phase turns out to be ineffective in terms of yield of the filtrate. Filtration in liquid phase is much efficient (Mercer *et al.*, 2008; Tsuda, personal communication). However, in our experience, the difficulty is found in avoiding re-aggregation during the process of drying; the surface tension. To solve this problem, here we report a new improved dispersion method consisting of a combination of aqueous filtering and the concept of a drying method used for scanning electron microscopic (SEM) samples; the critical point drying.

MATERIALS AND METHODS

MWCNT, reagent and equipments

MWCNT (Mitsui MWNT-7) was kindly donated by Mitsui & Co., Ltd., Tokyo, Japan for use in toxicity studies (Takagi *et al.*, 2008). Tert-butanol (TB) of guaranteed reagent grade was used (CAS: 75-65-0, Kanto Chemical Co., Inc., Tokyo, Japan). Metallic Sieve (pore size 25 μm mesh, Seishin Enterprise Co., LTD., Tokyo, Japan) was used for filtration. Miniature coin type vibration motors used in cellular phones (Model FM34F, T.C.P. Co, Tokyo Japan; 13,000 rpm 1.8m²/sec) are attached to the extended filler rim (5cm in depth, custom-made, Seishin Enterprise Co., LTD.) of the metallic sieve (cf. Fig. 1c) to gain high yield of filtrate. Chemistry diaphragm pumps and pumping systems (Model; MD4C NT+AK+EK, Vacuubrand, Wertheim, Germany) was used for sublimation of the frozen TB suspension and recovery of TB. Glass wares such as funnel, filtering bottle, trap bottle and silicon stoppers (Sansyo Co., Ltd., Tokyo, Japan), laboratory bottles (Pyrex®, Asahi Glass Co. Ltd., Tokyo, Japan), were used.

Dispersion method ("Taquann" method)

An outline flowchart is shown in Fig. 1. TB (melting point 25.69°C) was heated up to 60°C by a mantle heater (Sibata Scientific Technology Ltd., Saitama, Japan). It is advised not to use water bath; TB is highly hygroscopic and becomes difficult to freeze and sublimate. A volume of 200 ml of TB and 0.2 g of MWCNT were transferred to a 500 ml laboratory bottle and agitated to make crude suspension. The bottle was put into an ice bath, occasionally shaken by hand, until the suspension starts to freeze and becomes sherbet-like half frozen state and kneaded by a stainless steel spatula until it becomes evenly gray without clear crystals of TB (Fig. 1a), and then kept overnight at -25°C. To the frozen suspension, 500 ml of TB pre-heated to 60°C, was added, capped and shaken hard until the liquefied suspension becomes evenly dark brown to gray in color (Fig. 1b). The bottle was further heated up to 60°C by a mantle heater and the suspension was immediately applied to vibrating metal sieve for filtration (Fig. 1c). The filtrate was collected through a funnel into a 1,000 ml laboratory bottle. Immediately after the filtration, approximately 1,500 ml of liquid nitrogen was poured onto the filtrate in the bottle to snap freeze the suspension (Fig. 1d). Then, the bottle was connected to the pumping system and vacuumed until TB was totally sublimated; leaving dispersed MWCNT (T-CNT for Taquann-treated MWCNT) in the bottle. The MWCNT was collected by a cyclone-suction bottle using conduc-

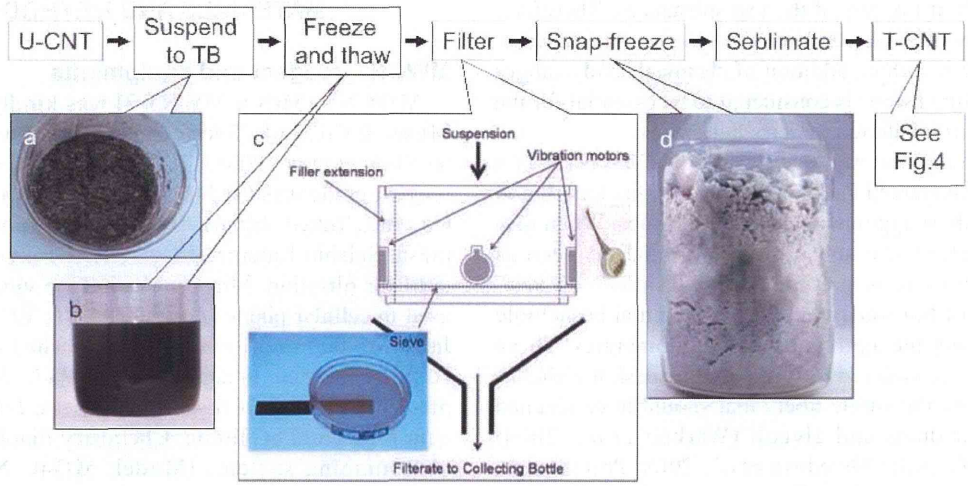

Fig. 1. Outline flowchart of the Taquann method. a) Half-frozen sherbet-like suspension of MWNT-7 kneaded (beaker was used for demonstration). b) Well-shaken liquefied suspension after adding 60°C TB (beaker was used for demonstration). c), Photograph of the sieve on a backlight box with a scale underneath (left inset), vibration motor (right inset), and a diagram of the filter unit with a filler extension and vibration motors. d) Snap-frozen filtrate.

tive silicon and aluminum tubing. In order to make a precise aliquot, a measured amount the collected T-CNT was resuspended to TB, and the suspension was aliquoted into proper containers, in this study into the newly designed cylindrical cartridge case (cf. Fig. 3), snap-frozen, and sublimated.

Aerosol generation system

An originally designed 105 L main exposure chamber (capacity of 16 mice per chamber), with a disposable electrostatic-free plastic bag inside, was prepared (Fig. 2, patent pending, manufactured by Sibata Scientific Technology Ltd.). Onto the plastic disposable top plate, a 20 L subchamber was connected with a 5 cm-diameter 10 cm long connecting pipe. To the subchamber, an injection port was connected, to which a newly designed cylindrical cartridge (manufactured by Sibata Scientific Technology Ltd.) containing dispersed T-CNT is loaded. The cartridge has a slide-valve air inlet at its base and four ejection holes at its top opening towards the subchamber lumen. The compressed air (0.8 M pascal) was injected five times with 0.2 sec duration and 10 sec interval to empty the T-CNT into the subchamber (Fig. 3). The carrier air flow from the subcamber to the main chamber was 15 L/min. Twenty-one cartridges were prepared for a two-hr exposure experiment, loading first two in 1 min for an initial boost and then one in every 6 min, resulting in generation of saw-tooth concentration wave with an average of 1.3 mg/m^3 (250 μg/cartridge) and 2.8 mg/m^3 (500 μg/cartridge).

Twelve C57BL/6NCrSlc male mice (SLC, Inc., Shizuoka, Japan), 10~11 weeks old, body weight of 23.8~30.8 g were placed in the cage suspended from the top plate of the inhalation chamber and exposed to 1 mg/m^3 of T-CNT for 2 hr a day for 5 days, lungs (excluding primary bronchi) were sampled and subjected to characterization of deposited fibers (see below).

The animal study was conducted in accordance with the Guidance for Animal Studies of the National Institute of Health Sciences under Institutional approval.

Real time particle counting and weight measurement

An optical particle counter (OPC) with a nominal detection limit of 300 nm (OPC-110GT, Sibata Scientific Technology Ltd.) and a condensation particle counter (CPC) with a nominal detection limit of 2.5 nm (ultrafine condensation particle counter 3776, Trust Science Innovation, MN, USA) were connected to the main chamber with a sample flow of 2.83 L (0.1cf) /min and 0.3 L/min respectively. The mass concentration of the chamber aerosol was calculated from the weight increase of polytetrafluoroethylene-glass fiber filter (Model T60A20, φ55mm, Tokyo Dylec Corp, Tokyo, Japan) after filtering the chamber aerosol by an Asbestos sampling pump (AIP-105, Sibata Scientific Technology Ltd.) at a rate of 1.5 L/min for 120 min (total of 180 L). Filter weight was measured by a microbalance (XP26V,

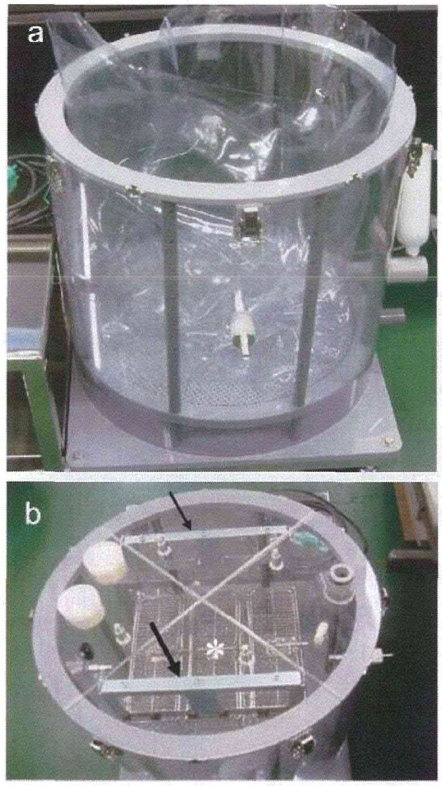

Fig. 2. Newly designed original inhalation chamber. a) Outer chamber and inner bag before top plate is in place. During operation, the space between the outer chamber and inner bag is negatively pressured to inflate the inner bag. B) Disposable top plate with tubing holes are placed on the chamber. The animal cages for 16 mice (asterisk) are suspended from the top place by a pair of hanger arms (arrows) (photo was taken without inner bag for better demonstration).

Fig. 3. A scheme of direct injection aerosol generation system. a) Upper inset shows the cut section of the injection cartridge (capacity; 23.5 ml). A slide valve opens when the cartridge is loaded to the subchamber. A measured amount of dispersed MWCNT is preloaded inside the cartridge shown in asterisk. b) Compressed air (Blue arrow 1) blows out the MWCNT through four small outlets of the cartridge into the subchamber (red arrows 3), where main flow air from the HEPA filtered inlet (blue arrow 2) mixes in. The air with the aerosol goes down the connection pipe to the main chamber (red arrow 4).

Mettler Toledo).

Characterization of the dispersed MWCNT

The T-CNT in TB suspension was mounted on a slide glass and observed under a light microscope using a pair of polarizing filters. Untreated MWCNT (U-CNT) from the bulk, 200 mg, was dispersed in to 500 ml of TB and sonicated for 30 min at 40W, 3.4 kHz (SU-3TH, Sibata Scientific Technology Ltd.) and observed.

A weight-measured aliquot of T-CNT was re-suspended, blotted on a Anopore™ Inorganic Aluminum Oxide Membrane Filters (Whatman GmbH, Dassel GE Healthcare, Hahnestrasse, Germany, pore size; 0.02 μm, φ13 mm, Anodisc 13) or a cellulose acetate/nitrocellulose membrane filter (MFTM- Millipore Membrane filters, 0.025 μm, φ13 mm, Merck Millipore, Billerica, MA, USA) and observed with a scanning electron microscope (SEM).

From the main chamber, the aerosol was collected at a rate of 5 L/min for 3 min on a Anopore™ Inorganic Aluminum Oxide Membrane Filters (Whatman GmbH, pore size; 0.1 um, Anodisc 25) joined to asbestos sampling pump (AIP-105, Sibata, Scientific Technology Ltd.). A scanning electron microscope (SEM) (VE-9800, Keyense Co., LTD., Osaka, Japan) was used for monitoring the details of the samples on the slide glasses and on the Anodiscs after osmium coating (HPC-1SW, Vacuum Device Inc., Ibaraki, Japan).

From the exposed mouse, lung lobes are collected and treated with lysis solution composed of 5 w/v% potassium hydroxide (Super Special Grade, Wako Pure Chemical Industries, Ltd., Osaka, Japan), 0.1w/v% Sodium dodecyl sulfate (SDS, for Biochemistry, Wako Pure Chemical Industries, Ltd.), 0.1 w/v% Ethylenediamine-N,N,N',N'-tetraacetic acid disodium salt dehydrate (EDTA 2Na, Dojindo laboratories, Kumamoto, Japan) and 2w/v% ascorbic acid (Super Special Grade, Wako Pure Chemical Industries, Ltd.) in ultra-pure water, dissolved at 80°C (Fig. 10b). Lung samples (approx. 200 mg) and 1.8 ml of

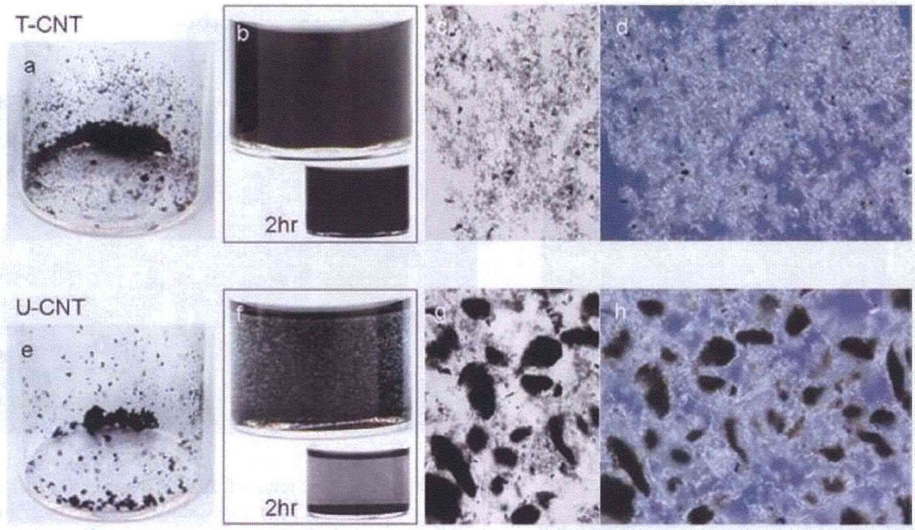

Fig. 4. Taquann-treated carbon nanotube (T-CNT) and untreated bulk carbon nanotube (U-CNT). a) final fine and dry powder of Taquann-treated MWCNT. b) Resuspended T-CNT to TB and placed for 5 min and 2 hr; T-CNT suspension is stable, compared to U-CNT, c) light microscopic view of the resuspended T-CNT on a slide glass, and d) under polarized light. e) course powder of U-CNT, f) Resuspended U-CNT to TB and placed for 5 min and 2 hr. g) light microscopic view of the resuspended U-CNT on a slide glass, and d) under polarized light. (diameter of the vials in a), b), e) and f) is 2.3 cm)

lysis solution in a centrifuge tube (DNA LoBindid tube 2.0 ml, Eppendorf, Hamburg, Germany) was incubated at 80°C for approx. 24 hr in an oven (HV-100, Funakoshi Co., Ltd., Tokyo, Japan), centrifuged at 20,000 g for 1 hr at 25°C (MX-207, Tomy Seiko Co., Ltd., Tokyo, Japan), and the pellet containing MWCNTs and SDS crystals was recovered. 1.8 ml of 70% ethanol was added to the tube and incubated at 80°C for 30 min to dissolve SDS crystals and centrifuged at 20,000 g for 1 hr at 25°C. 100 µl of 1w/w% Triton®X-100 (MP Biomedicals, Inc., Solon, OH, USA) was added to the pellet and dispersed by pipetting. One microliter of the suspension was placed on an inorganic aluminum oxide membrane filter (Anodisc 13, 0.02 µm φ13mm, Whatman GmbH) or the cellulose acetate/nitrocellulose membrane filter and filtrated on a funnel shape glass filter (SANSYO Co., LTD., Tokyo, Japan). The filter was dried at room temperature and osmium coated for SEM. For a reference of extraction efficiency, lung sample from untreated mouse was spiked with 1 µg T-CNT and measured alongside.

Lung tissue from eight mice were fixed with buffered 10% formalin (four with and four without inflation), paraffin embedded and processed routinely for H&E stained histology slides, and observed under a light microscope with or without polarizing filters (Olympus BX50 microscope with DP-70 image system, Olympus Corporation, Tokyo, Japan).

RESULTS

Characteristics of "Taquann"-dispersed MWCNT

Macroscopic and light microscopic views of the final product, the dried MWCNT after sublimation, i.e. "Taquann"-dispersed MWCNT (T-CNT) and, for comparison, untreated MWCNT from the bulk (U-CNT) are shown in Fig. 4. The powder of T-CNT is finer compared to U-CNT (Fig. 4a). The T-CNT resuspended very well to TB (Fig. 4b) and other solvents including 0.1 w/v% Sodium dodecyl sulfite and 0.1 w/v% Sodium dodecylbenzene sulfonate (not shown). Light microscopically, the resuspended T-CNT consists mostly of dispersed single fibers with smaller numbers of small aggregates corresponding to the mesh size of the metal sieve (Figs. 4c, 4d), whereas U-CNT was a mixture of large aggregates/agglomerates and single fibers among them (Figs. 4g, 4h). The T-CNT fibers slowly precipitated in the medium (cf. Figs. 4b and f), and are easily resuspended by gentle agitation. The yield of the T-CNT was approximately 5% of the U-CNT in weight. Re-filtration of the residue on the sieve resulted in negligible yield. The low power SEM views of the TB-resuspended T-CNT and U-CNT are shown in Fig. 5.

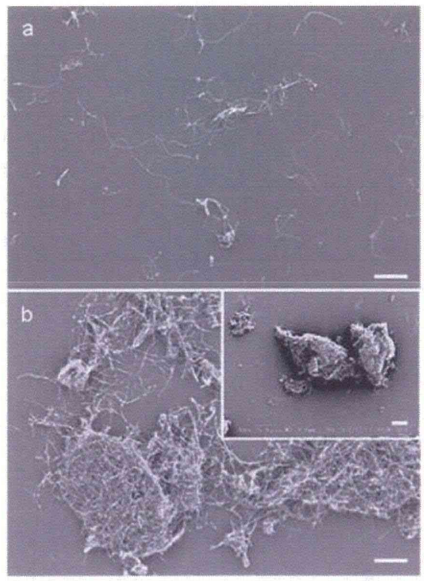

Fig. 5. Scanning electron microscopy of T-CNT and U-CNT re-suspended in TB. a) T-CNT consists mainly of dispersed single fibers with few small aggregates/agglomerates smaller than the mesh size of the sieve, SEM x 1,000. b) U-CNT showing mixture of single fibers and large aggregates/agglomerates, SEM x 1,000. The length and width distribution of the single fibers of T-CNT were virtually identical to those of U-CNT. Inset; Lower power view to demonstrate larger aggregates/agglomerates measuring up to 300 μm in major axis SEM x 400. (scale bars are 10 μm)

Again, the majority of the particles of the T-CNT were the dispersed single fibers. The length and width distribution of single fibers counted on these SEM images are shown in Fig. 6. The length and width distribution was similar between single fibers of T-CNT and U-CNT, indicating that the mechanical shortening of the fibers is negligible for Taquann method.

The number of fibers per 10, 1 and 0.1 μg weight of T-CNT with length distribution was counted on SEM images (measured number of fibers are 959, 246, and 45 per designated area for calculation, respectively). The number of fibers calculated was 2.1 x 10^7/10 μg 4.1 x 10^6/1 μg and 3.3 x 10^5/0.1 μg. The distribution of the fiber length was similar to that shown in Fig. 6a, and the average length was 7.5 ± 4.7 μm (max 34 μm), 8.7 ± 6.4 μm (max 42 μm), and 7.0 ± 5.4 μm (max 26 μm) respectively. As a whole, T-CNT has roughly 3 x 10^6 fibers per 1 μg, mean length of approximately 7 μm with a length range up to 50 μm with a median of approximately 6.5 μm.

"Taquann"-dispersed MWCNT in the inhalation chamber

The T-CNT aerosol generated at an average concentration of 1 mg/m³ was sampled on the Anodisc and observed by a SEM (Fig. 7). The aerosol was composed mainly of well-dispersed single fibers and some small tangles of fibers admixed with a relatively small amount of non-fibrous particles.

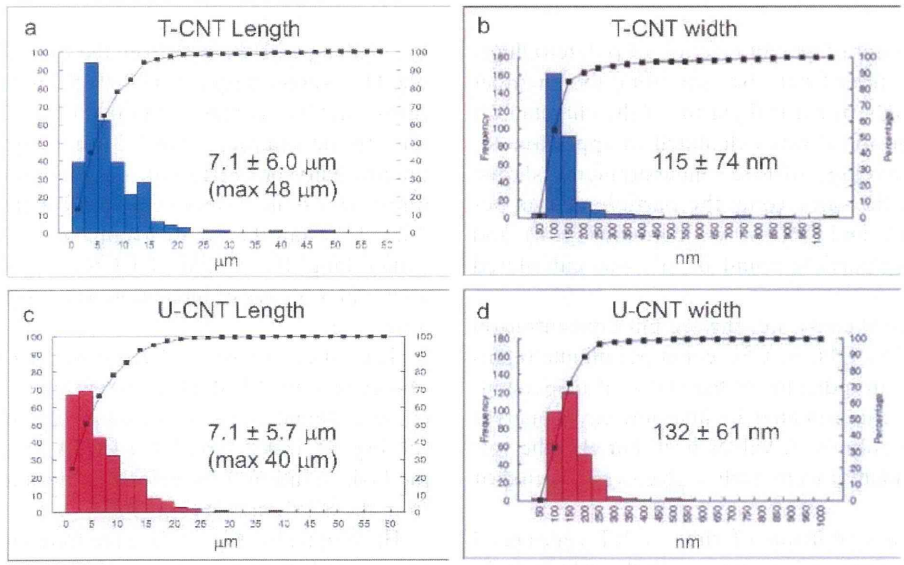

Fig. 6. Length and width of single fibers in T-CNT and U-CNT (measured by SEM on TB-resuspended samples). a) Length distribution and b) width distribution of Taquann-treated MWNT-7. c) Length distribution and d) width distribution of single fibers in the mildly sonicated suspension of the bulk MWNT-7 (mean ± s.d., n = 304 each).